Chinese Journal of
POLYMER SCIENCE

RESEARCH ARTICLE

https://doi.org/10.1007/s10118-026-3634-5
Chinese J. Polym. Sci. **2026**, *44*, 2282–2293

A Phosphorus/Nitrogen-containing Phosphaphenanthrene Derivative as Flame Retardant for Poly(lactic acid)

Shan Lin, Hong-Yan Zhu, Chun-Meng You, and Da-Ming Ban*

School of Chemistry and Materials Science, Guizhou Normal University, Guiyang 550025, China

Abstract As a bio-based and biodegradable aliphatic polyester, poly(lactic acid) (PLA) holds great promise as a sustainable alternative to conventional petroleum-derived plastics. However, its inherent flammability remains a critical barrier to its use in advanced polymer composites requiring stringent fire-safety standards. In this work, a phosphorus/nitrogen-containing flame retardant (FMPO) was synthesized from melamine (MEL), formaldehyde (FA) and 9,10-dihydro-9-oxa-10-phosphaphenanthrene-10-oxide (DOPO) at a 1:1 molar ratio to serve as a flame-retardant modifier for PLA. The results demonstrated that with only 1 wt% FMPO loading, the PLA composite achieved a UL-94 V-0 rating, and the limiting oxygen index (LOI) increased significantly to 33.2% by 5 wt%. At the same flame retardant content, PLA/5MEL only showed a LOI of 26.8% and a UL-94 V-2 rating. Meanwhile, the mechanical strength of PLA/5FMPO was significantly improved, exhibiting 136% and 41% higher impact strength and tensile strength than PLA/5MEL. The analysis of char residue and incomplete combustion products revealed that FMPO exhibits a bi-phase flame-retardant effect, characterized by gaseous-phase inert-gas dilution and radical quenching, along with a condensed-phase thermal barrier from the carbon layer. This study demonstrates an efficient and sustainable strategy for fabricating high-performance, flame-retardant PLA materials through P/N synergistic fire resistance.

Keywords Poly(lactic acid); Phosphaphenanthrene; Flame retardants; Mechanical properties; Flame retardancy mechanism

Citation: Lin, S.; Zhu, H. Y.; You, C. M.; Ban, D. M. A phosphorus/nitrogen-containing phosphaphenanthrene derivative as flame retardant for poly(lactic acid). *Chinese J. Polym. Sci.* **2026**, *44*, 2282–2293.

INTRODUCTION

Conventional petroleum derived polymers, including plastics, rubbers, and fibers, have brought tremendous convenience to modern life owing to their versatility and processability.[1] Nevertheless, these materials are responsible for substantial resource depletion and long-term environmental accumulation across their entire lifecycle from production and use to disposal.[2] In response to environmental challenges and the pressure to deplete petrochemical resources, bio-based and biodegradable polymers have emerged as promising alternatives, among which poly(lactic acid) (PLA) is one of the most widely studied candidates for sustainable polymer composites.[3–5]

PLA is sourced from plant-based materials such as corn, which alleviates dependence on finite petroleum feedstocks.[6] Furthermore, its inherent biodegradability allows complete decomposition into CO_2 and H_2O under specific composting conditions, thereby preventing long-term environmental accumulation.[7] PLA further offers both robust mechanical performance and biocompatibility. These attributes have driven its adoption in applications ranging from 3D printing to biomedical devices and packaging.[8–10] However, the elemental composition of PLA and its molecular chain structure result in a flammability defect. Upon exposure to a flame, PLA ignites rapidly and tends to produce melt-dripping, which notably increases the risk of fire spread and poses a direct threat to personal safety.[11–13] These characteristics severely restrict its use in fields with stringent fire-safety requirements, including electronics, transportation, and construction materials. Therefore, the development of highly efficient flame retardants for PLA is crucial for broadening its application scope.

The directly addition of flame retardants to PLA materials is a simple and cost-effective method for achieving flame retardancy.[14–17] Halogen-based flame retardants, which are widely used to suppress combustion, release highly toxic and persistent organic pollutants such as hydrogen halides and dioxins during fire incidents. These emissions have introduced severe secondary hazards to ecosystems and human health.[18] In the category of halogen-free alternatives, phosphorus-based flame retardants have emerged as the most promising option owing to their variety, minimal toxicity, and superior flame suppression capability.[19,20] Among these compounds, the DOPO (9,10-dihydro-9-oxa-10-phosphaphenanthrene-10-oxide) and its structural analogs have drawn substantial research attention because of their exceptional fire retardancy performance.[21,22] Pei *et al*.[23] prepared a phosphazene flame retardant (DOPO-PHBA) by structurally modifying DOPO with

* Corresponding author, E-mail: bdaming@gznu.edu.cn
Received January 4, 2026; Accepted February 25, 2026; Published online May 14, 2026

p-hydroxybenzaldehyde to enhance the thermal stability of PLA. Although DOPO-PHBA demonstrated superior flame retardancy over DOPO, it required an epoxy chain extender to maintain its mechanical properties. To address these problems, researchers have found that incorporating additional flame-retardant elements into DOPO is highly effective in improving flame-retardant efficiency.[24] Among these, the phosphorus-nitrogen synergistic flame retardants are the most adapted for PLA. For example, Wang *et al.*[25] added a DOPO derivative (DOPO-NH_2) with an amino terminal group was added to PLA to optimize flame retardancy. The results showed that with 5 wt% DOPO-NH_2 the PLA composites could reach UL-94 V-0. Meanwhile, the composites also retained their mechanical properties, thanks to the low dosage of additive and enhanced interfacial adhesion from hydrogen bonding.

Based on the aforementioned dual environmental and safety challenges, a phosphorus/nitrogen-containing flame retardant, N^2-[(10-dihydro-9-oxa-10-phosphaphenanthrene-10-oxide) methylene]-1,3,5-triazine-2,4,6-triamine (FMPO), was synthesized. Then, FMPO was added to biodegradable PLA to enhance the flame resistance, with PLA composites containing 5 wt% MEL as a control. A comprehensive evaluation of the flame retardancy, thermal behavior and mechanical performance was performed. The mechanism is discussed in detail. This research offers a novel material solution for PLA fire safety improvement and advances the development of flame-retardant technologies.

EXPERIMENTAL

Materials

Melamine (MEL, analytical grade, 99%) was obtained from Shanghai Yuanfan Additives Factory (Shanghai, China). Formaldehyde solution (FA, analytical grade) with a concentration of 37%–40% was purchased from Xilong Scientific Co., Ltd. (Guangdong, China). Anhydrous ethanol (analytical grade, 99.7%) was purchased from Sinopharm Chemical Reagent Co., Ltd. (Shanghai, China). DOPO with 99.5% purity was obtained from Shenzhen Jinlong Chemical Co., Ltd. (Guangdong, China). Polylactic acid (PLA, 4043D) with a density of 1.24 g/cm^3 was purchased from NatureWorks Co., Ltd. (USA).

Synthesis of FMPO

A three-necked flask, which was outfitted with an overhead mechanical stirrer and condensation reflux system, was charged with melamine (0.1 mol), formaldehyde (0.1 mol), and anhydrous ethanol (120 mL). The reaction mixture was heated to 85 °C with stirring, and the conditions were held constant for 30 min. Subsequently, DOPO (0.1 mol) was introduced, and the mixture was subjected to a stirring regime at 85 °C for 2 h. The precipitated crude product was washed three times with anhydrous ethanol, and the collected solid was then dried in an oven at a constant temperature to achieve a constant weight. This procedure afforded the final product, FMPO, as a white powder (43.5% yield). The reaction pathway is shown in Scheme 1.

Preparation of PLA/FMPO Composites

FMPO at varying mass ratios was added to the PLA matrix through mechanical blending, followed by preheating at 180 °C for 3 min in a torque rheometer. The preheated mixture was then blended for 5 min at 180 °C at a rotor speed of 80 r/min. The resulting plastic block was crushed, hot-pressed, and melt-formed in a platen vulcanizer at 170 °C and 10 MPa for 6 min. The material was trimmed according to sample dimensions. The composite formulations are listed in Table 1.

Characterizations

Infrared spectroscopic analysis of DOPO, FMPO, and MEL was performed using a Nicolet iS5 Fourier-transform infrared (FTIR) spectrometer (Thermo Fisher Scientific, USA). Samples were prepared by the KBr pellet method, with spectra recorded in the wavenumber range of 4000–400 cm^{-1}.

The NMR (^{1}H, ^{13}C, and ^{31}P) spectra were recorded on a Bruker Avance-600 spectrometer (Bruker, Germany), employing deuterated methanol (CD_3OD) as the solvent for sample preparation.

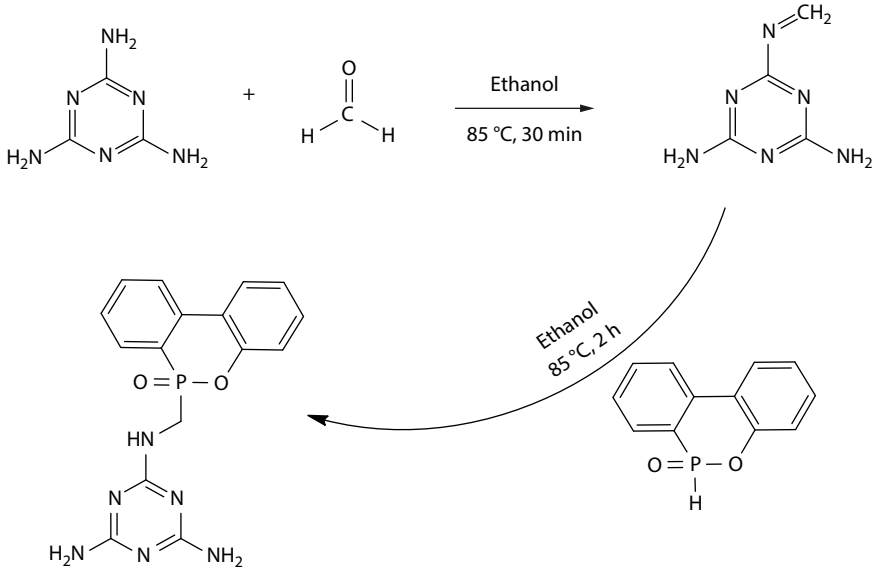

Scheme 1 The preparation process of FMPO.

https://doi.org/10.1007/s10118-026-3634-5

Table 1 Composition, LOI and UL-94 results for PLA composites.

Sample	Mass fraction (%)				LOI (%)	UL-94		
	PLA	MEL	FMPO	P content		t_1+t_2 (s)	Rating	Flame dripping
PLA	100	0	0	0	21.6	>30	NR	Heavy dripping
PLA/5MEL	95	5	0	0	26.8	8.5	V-2	Heavy dripping
PLA/1FMPO	99	0	1	0.0874	26.2	6.2	V-0	Heavy dripping
PLA/2FMPO	98	0	2	0.1748	29.5	4.5	V-0	Dripping
PLA/3FMPO	97	0	3	0.2622	30.1	3.6	V-0	Slight dripping
PLA/4FMPO	96	0	4	0.3496	32.0	2.2	V-0	Slight dripping
PLA/5FMPO	95	0	5	0.4370	33.2	0	V-0	Slight dripping

Thermogravimetric analysis (TGA) was performed using a STA 409 PC/PG instrument (Netzsch, Germany) under a nitrogen atmosphere. The samples were subjected to linear temperature programming at 20 °C/min from 40 °C to 700 °C in alumina crucibles.

The limited oxygen index (LOI) was determined according to ASTM D-2863 on a JF-3 device (Jiangning, China), with samples of dimensions 120 mm × 6.5 mm × 3.2 mm.

UL-94 vertical burning ratings were evaluated based on ASTM D-3810 using a CFZ-6 vertical flame tester (Jiangning, China), with specimens sized at 120 mm × 13 mm × 3.2 mm.

Cone calorimeter test (CCT), conducted in accordance with ISO 5660-1 at a heat flux of 50 kW/m^2, was used to evaluate the combustion characteristics of 100 mm × 100 mm × 3 mm composite specimens using an FTT 0007 instrument (FTT, UK).

The microstructure of the gold-coated char residues was analyzed by scanning electron microscopy (SEM) using a GeminiSEM 360 instrument (Zeiss, Germany) at an accelerating voltage of 15 kV.

X-ray photoelectron spectroscopy (XPS) measurements were performed on the char residue obtained after the CCT using an EscaLab 250Xi spectrometer (Thermo Fisher Scientific, USA). The analysis was conducted with an Al Kα excitation source ($h\nu$=1486.6 eV) operated at 6 mA.

The real-time composition of the pyrolysis gases was monitored using a simultaneous thermal analyzer (STA 6000, PerkinElmer, USA) coupled with a Fourier transform infrared spectrometer (Frontier, PerkinElmer, USA).

The Raman spectra of the post-CCT residues were recorded on a Renishaw inVia 2000 spectrometer (Renishaw, UK) using a 532 nm laser. The spectral acquisition was performed over a range of 50–4000 cm^{-1}.

The tensile properties were tested according to GB/T 1040.2-2006 using a CMT 4202 universal testing machine (Dongte, China) at a crosshead speed of 50 mm/min on specimens measuring 150 mm × 12 mm × 3 mm. The impact properties were evaluated on a ZBC 1400-B impact tester (Mester, China) using specimens with dimensions of 100 mm × 10 mm × 4 mm.

RESULTS AND DISCUSSION

Structural Characterization of FMPO

The FTIR and NMR (^{1}H, ^{13}C, and ^{31}P) spectroscopy were used to characterize the chemical structure of FMPO. The FTIR spectra of DOPO, MEL and FMPO are compared in Fig. 1(a). The absorption bands of DOPO at approximately 2385, 1240, and 754 cm^{-1} corresponded to the characteristic peaks of the P—H bond, P=O bond, and P—O—C structure, respectively.[26] As for the FTIR spectrum of MEL, the four sharp —NH_2 stretching peaks in the 3466–3113 cm^{-1} region.[27] Moreover, the absorption near 1650 cm^{-1} corresponds to the C=N stretch in the triazine ring.[28,29] In the infrared spectrum of FMPO, the characteristic —NH_2 absorption was located between 3466 and 3113 cm^{-1}, and the distinctive peaks of the triazine ring were also preserved. The —CH_2 groups give rise to two distinct signals at 2978 and 2895 cm^{-1}, identified as symmetric and asymmetric stretching vibrations, respectively, while the characteristic signal at approximately 1354 cm^{-1} corresponds to the C—N bond absorption. Furthermore, the appearance of a signal at approximately 1280 cm^{-1}, which is characteristic of the P=O bond, confirmed the successful incorporation of the phosphophenanthrene group.[30,31]

Additionally, ^{1}H-NMR spectroscopy was performed to confirm the successful synthesis of FMPO. In Fig. 1(b), two signals are observed at 3.6 and 6.7 ppm, attributed to the —CH_2 and N—H protons, respectively, 6.9–8.0 ppm could be identified as the aromatic protons.[32] Furthermore, the integration ratio from the spectrum agrees with the theoretical structure. Additionally, the ^{13}C-NMR spectrum of FMPO displayed 16 signals, which is consistent with the four unique carbon environments in the theoretical structure. The peaks of the carbon atoms in the triazine ring and C—O were observed at 153.7 and 140.5 ppm. And signals at 116.5–131.3 ppm (benzene ring carbons) and 56.9 ppm (—CH_2 carbon) were observed. The ^{31}P-NMR spectrum of FMPO showed a signal at 17.5 ppm, assigned to the phosphorus atom of the DOPO moiety. Nevertheless, there were additional signal peaks, which might have been caused by the rigid groups in the FMPO molecule. The steric hindrance from these groups can result in stereoisomers of the phosphorus peak with unequal intensities. In summary, these results confirmed that FMPO has a presumptive molecular structure.

Thermal Stability Analysis

Fig. 2 shows the TG and DTG behaviors of the materials under the N_2 atmosphere, and the key thermogravimetric data are compiled in Table 2. The degradation processes of both pure PLA and the modified composite followed a single-step degradation, indicating that MEL and FMPO did not altered the degradation process of PLA. The addition of FMPO lowered both $T_{5\%}$ (initial decomposition temperature) and T_{max} (maximum weight loss temperature). This is due to the inherent thermal lability of the P—O—C and P—C in the phosphaphenanthrene structure, which begins to break at high temperatures ahead of the matrix, leading to premature degradation of PLA composites.[33,34] Nevertheless, FMPO incorporation enhanced char formation, as evidenced by the higher residue at 700 °C

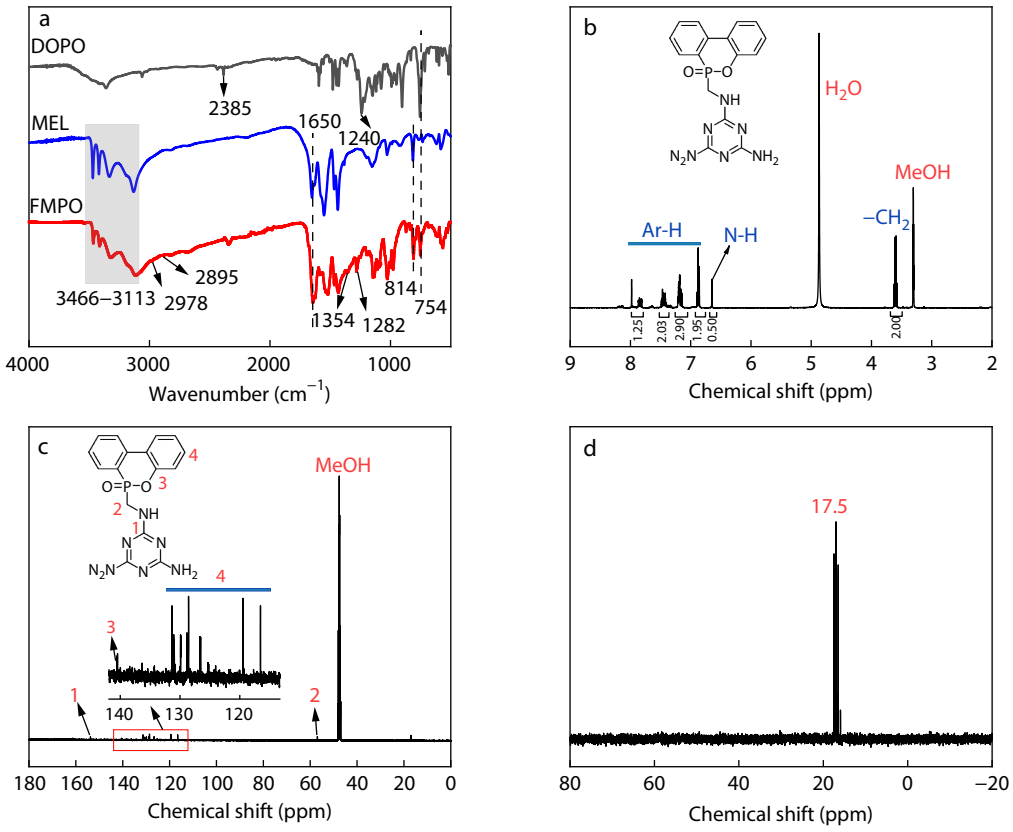

Fig. 1 (a) FTIR spectra of DOPO, MEL, and FMPO, (b) ^{1}H-, (c) ^{13}C-, and (d) ^{31}P-NMR spectra of FMPO.

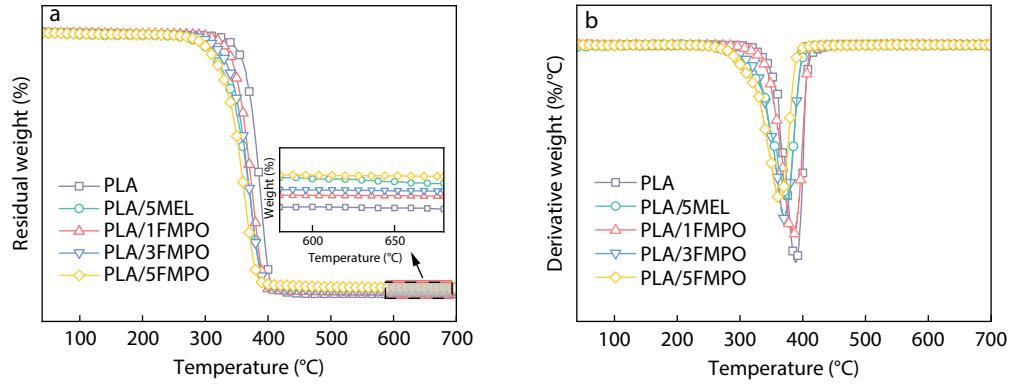

Fig. 2 (a) TG and (b) DTG thermograms of PLA composites.

Table 2 The key thermogravimetric data of PLA composites.

Sample	$T_{5\%}$ (°C)	$T_{50\%}$ (°C)	T_{max} (°C)	R_{700} (%)
PLA	345.2	384.0	389.0	0.39
PLA/5MEL	296.3	364.2	374.2	2.16
PLA/1FMPO	329.7	369.9	383.9	1.33
PLA/3FMPO	312.2	365.4	372.4	1.68
PLA/5FMPO	298.2	356.1	361.0	2.75

and the concurrent decrease in the maximum mass loss rate. Furthermore, at the same additive content, the residual mass of PLA/5FMPO (2.75%) was higher than that of PLA/5MEL (2.16%), suggesting that PLA/FMPO exhibited a superior charring ability.

Flame Retardancy of PLA Composites

The flame-retardant performance of the PLA composites containing FMPO or MEL was evaluated *via* limiting oxygen index (LOI) and UL-94 vertical burning tests. The specific test parameters are listed in Table 1, and the corresponding burning behaviors are visually documented in Fig. 3. As shown in Fig. 3, pure PLA burned rapidly upon ignition, accompanied by substantial flaming drips that ignited the underlying absorbent cotton, thus

receiving only an NR rating in the UL-94 test. The low LOI value of 21.6% further confirms the inherent flammability of the material. Notably, the LOI value of the composite with only 1 wt% FMPO was comparable to that of PLA/5MEL. However, the melt drips from PLA/1FMPO self-extinguished before contacting the absorbent cotton. This process effectively separated the heat from the pyrolysis zone of the material, enabling the composite to achieve a UL-94 V-0.[35] In contrast, with their melt drips lacking self-extinguishing capability, PLA/5MEL produced continuously burning drips that ignited the cotton, which led to a UL-94 V-2. As the FMPO loading increased, the LOI showed marked improvement. Upon reaching the maximum addition of the flame retardant (5 wt%), the LOI value for PLA/5FMPO significantly increased to 33.2%, which represented an approximate 53.7% enhancement compared to that of neat PLA. Furthermore, during the vertical burning test, the specimen proved challenging to ignite and demonstrated minimal dripping. This suggests that the addition of FMPO effectively imparted significant flame retardancy to the PLA composites.

The combustion behavior of the polymer composites under a defined heat flux was comprehensively characterized using a cone calorimeter test (CCT), a method that shows a well-recognized correlation with real-fire scenarios. Fig. 4 displays the corresponding curves for HRR (heat release rate), THR (total heat release), SPR (smoke production rate), and TSP (total smoke production). The key parameters listed in Table 3 include Pk-HRR (peak heat release rate). The data show that the ignition time (TTI) decreased to 30 s after adding 5 wt% MEL, whereas it increased to 46 s with the addition of 2 wt% FMPO. This occurred because the PLA/MEL composite exhibited inferior thermal stability compared with neat PLA, leading to its premature decomposition at lower temperatures. In contrast, the addition of a small amount of FMPO retarded this effect and increased the heat resistance of the composites. As shown in Fig. 4 and Table 3 relative to pure PLA, the SPR, TSR, and average CO production (Av-COY) of the PLA/FMPO composites slightly increased, while the THR and average CO_2 production (Av-CO_2Y) were decreased. These changes may originate from the incomplete combustion of the composite after the formation of an expanded char layer. Compared with the results of PLA/5MEL and PLA/2FMPO, the HRR, THR, SPR and TSR of PLA/2FMPO were significantly reduced. On the one hand, this was assigned to the decomposition of FMPO, which produces PO• radicals that effectively capture the highly reactive H• and OH• radicals from the decomposing PLA. On the other hand, NH_3 and N_2 released from the triazine ring dilution diluted the combustible gases. The combination of these factors reduced smoke emission. During this process, FMPO exhibited a significant flame-retardant effect in both the gas and condensed phases within the composite system.

Analysis on Residual Char

Studying the residual char offers crucial insights into the condensed-phase flame retardant mechanisms. Accordingly, char samples from after CCT were characterized using complementary analytical techniques, including SEM, XPS and Raman spectroscopy.

Figs. 5(a)–5(c) present a comparison of the macroscopic char residues for pure PLA, PLA/5MEL, and PLA/2FMPO composites. The digital images showed that pure PLA left almost no residue, whereas the residual carbon of PLA/5MEL was overall fluffy, with abundant pores and cracks present on the char layer surface. After adding 2 wt% FMPO, the char residue in this sample was evenly distributed at the bottom layer. Although the number of char layers was lower than that of PLA/5MEL, the char exhibited greater compactness and higher density.

To examine the microstructure, SEM was used to characterize the char residues of the PLA/5MEL, PLA/2FMPO, and PLA/5FMPO composites after CCT, as shown in Figs. 5(d)–5(i). The surface of the PLA/5MEL composite was characterized by extensive cracking and porosity, as observed by SEM. Moreover, it was noteworthy that the presence of prominent, ruptured pores can be seen on the char surfaces, marked by red dashed circles in Fig. 5(d). This phenomenon is attributed to

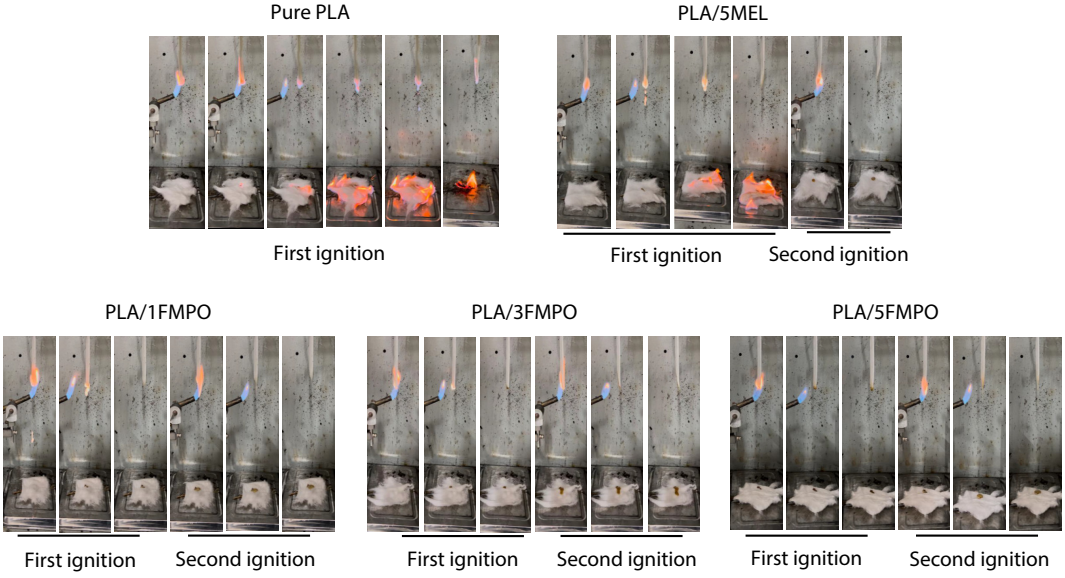

Fig. 3 Digital photographs of UL-94 tests.

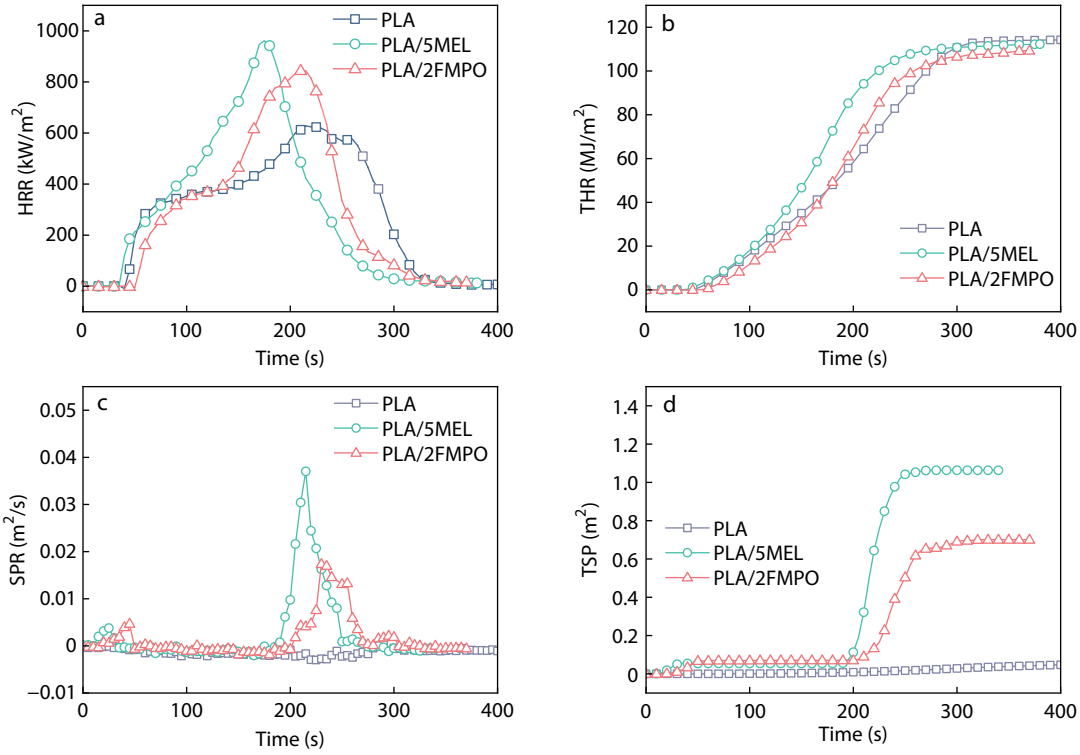

Fig. 4 (a) HRR, (b) THR, (c) SPR, and (d) TSP curves of the PLA composite.

Table 3 The data of CCT of PLA composites.

Sample	TTI (s)	Pk-HRR (kW/m^2)	THR (MJ/m^2)	TSP (m^2)	Av-COY (kg/kg)	Av-CO_2Y (kg/kg)	Av-EHC (MJ/kg)	Residue (%)
PLA	33	627.5	114.3	0.04	0.023	1.35	14.55	0.01
PLA/5MEL	30	961.8	112.3	1.03	0.036	1.27	13.31	1.7
PLA/2FMPO	46	844.6	109.3	0.64	0.038	1.16	12.81	0.7

the high loading of MEL in the matrix, which releases a substantial volume of gas upon heating. The gas becomes trapped within the cracked char layer, resulting in large internal pores and a hollow structure. In contrast, the char residue of PLA/2FMPO exhibited a honeycomb-like morphology with a reduction in both the number and size of pores. As can be seen from Figs. 5(h)–5(i), the char surface of PLA/5FMPO displayed an even more continuous and dense morphology, with extremely fine pores and excellent integrity. Consequently, compared to the internally hollow char structure of PLA/5MEL, the carbonized products of PLA/FMPO demonstrated a higher degree of cross-linking. Furthermore, as the FMPO content increased, the char structure progressively evolved from loose and porous to dense, leading to a significant enhancement in thermal insulation performance.[36,37]

In the Raman spectrum (Fig. 6), two characteristic bands are observed: the D band (1358 cm^{-1}) and the G band (1593 cm^{-1}), which are characteristic of amorphous and graphitized carbon, respectively.[38,39] The degree of graphitization was characterized by the signal integration ratio of these two peaks (I_D/I_G), where a lower I_D/I_G value signifies a more ordered carbon structure with resulting superior thermal insulation properties.[40] The I_D/I_G values decreased in the following order: PLA (4.6) > PLA/5MEL (4.3) > PLA/2FMPO (3.1). Evidently, all modified PLA thermosets exhibited consistently lower I_D/I_G ratios than pure PLA, confirming the efficacy of both MEL and FMPO in enhancing char graphitization. Furthermore, PLA/2FMPO demonstrated superior graphitic ordering relative to PLA/5MEL, suggesting that FMPO facilitated the development of a robust carbon shield, thereby leading to more effective flame suppression. In addition, these results were in accordance with the microstructural observations from SEM.

The chemical composition and electronic states of the residual char were analyzed using XPS, with the results presented in Fig. 7. The survey XPS spectra of the char residues of pure PLA, shown in Fig. 7(a), identified nitrogen (N) in the respective char residues of PLA/5MEL and PLA/2FMPO. Notably, the PLA/2FMPO sample also exhibited a peak at 134 eV corresponding to phosphorus (P), indicating that both P and N acted synergistically to enhance the solid-phase protective barrier. This synergism promotes the formation and stability of the char layer, which improved its isolation effect. The C 1s spectrum of PLA exhibited three peaks at around 284.7, 286.7, and 288.9 eV, representing the C—C/C—H, C—O, and C=O bonds, respectively.[41,42] A new peak emerged at 285.6 eV in the C 1s spectrum upon adding MEL or FMPO. This signal, attributable to C—N bonds, suggests the formation of nitrogen-containing char through the cleavage of the triazine ring in melamine during combustion. In the N 1s spectrum, the signal at 398.7 eV is assigned to C—N/C=N, and that at 400.6

https://doi.org/10.1007/s10118-026-3634-5

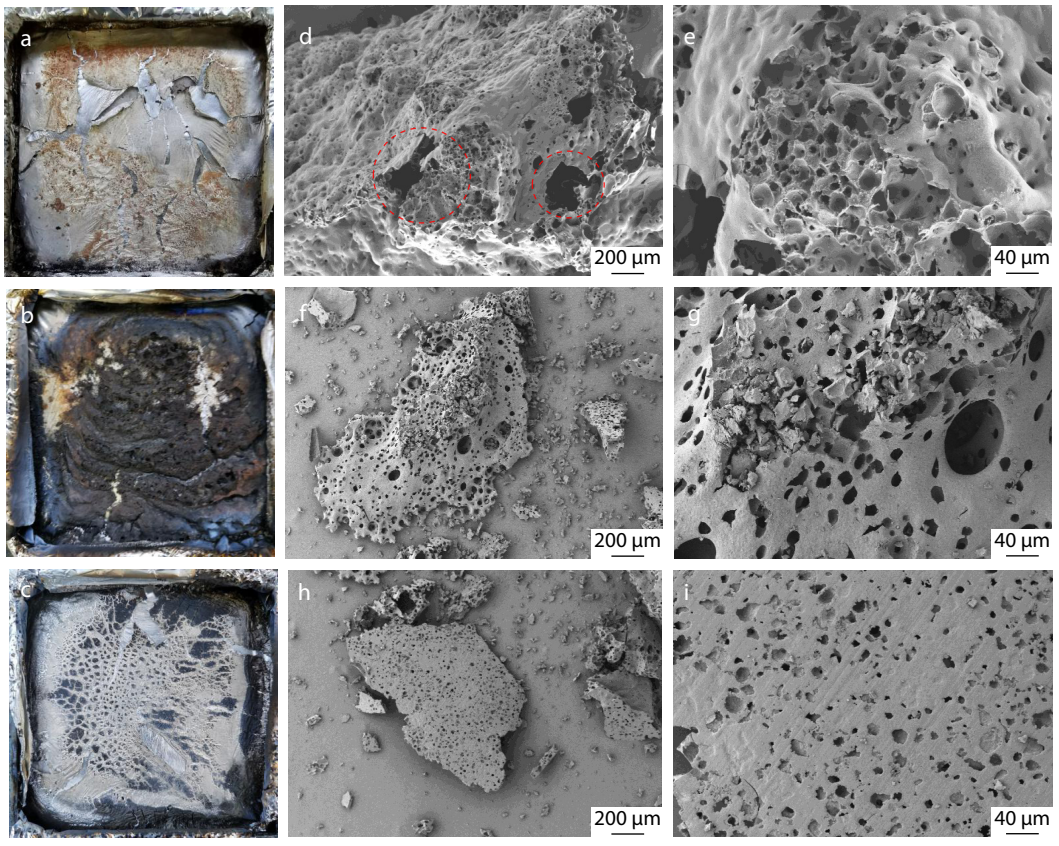

Fig. 5 Digital photographs after CCT: (a) pure PLA, (b) PLA/5MEL, (c) PLA/2FMPO. SEM images of residual carbon after CCT: (d) PLA/5MEL (200 μm), (e) PLA/5MEL (40 μm), (f) PLA/2FMPO (200 μm), (g) PLA/2FMPO (40 μm), (h) PLA/5FMPO (200 μm), (i) PLA/5FMPO (40 μm).

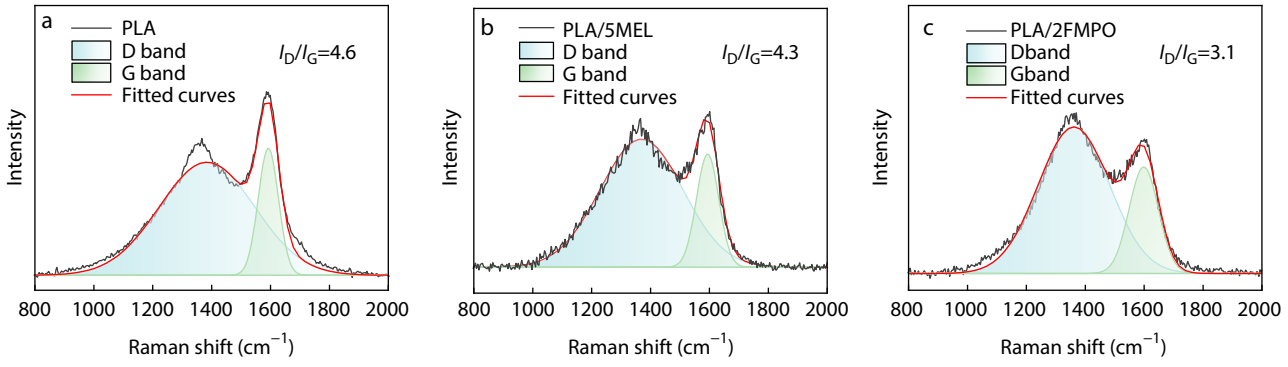

Fig. 6 Raman spectra of PLA composites: (a) pure PLA, (b) PLA/5MEL, (c) PLA/2FMPO.

eV to N—H. Correspondingly, the P 2p spectrum displays two components at 133.6 eV (P=O) and 134.7 eV (P—O—C). These findings suggest that the generation of isocyanic acid, metaphosphoric acid, and H_3PO_4 during the pyrolysis of FMPO promotes substrate dehydration and charring, which results in the accelerated establishment of a compact char barrier that isolates the flame and combustible gases from the surrounding environment.

Analysis of Gaseous Products

TG-IR serves as a reliable method for characterizing the gaseous decomposition products generated throughout the degradation process. As shown in Fig. 8(a), the primary volatile species identified during the pyrolysis of pure PLA thermosets included: H_2O (3582 cm^{-1}), hydrocarbons (2948 cm^{-1}), RCHO (2742 cm^{-1}), CO_2 (2360 cm^{-1}), CO (2186 cm^{-1}), C=O (1790 cm^{-1}), and C—O—C (1104 cm^{-1}).[43–45] Apparent from the FTIR spectral comparison, the signals corresponding to gaseous decomposition products were consistently weaker for PLA/2FMPO than for pure PLA. In the cases of PLA/2FMPO and PLA/5MEL, the signals of NH_3 appeared at 930 cm^{-1} for both. This observation suggests that both MEL and FMPO release inert gases, which suppress the level of flammable volatiles and simultaneously dissipate heat. Moreover, the FTIR spectrum of PLA/2FMPO showed an absorption near 750 cm^{-1}, attributable to P—O—C, signifying that the phosphorus-containing radicals participated through a radical quenching mechanism.

Flame-retardant Mechanisms

Based on these analytical findings, a possible flame-retardant

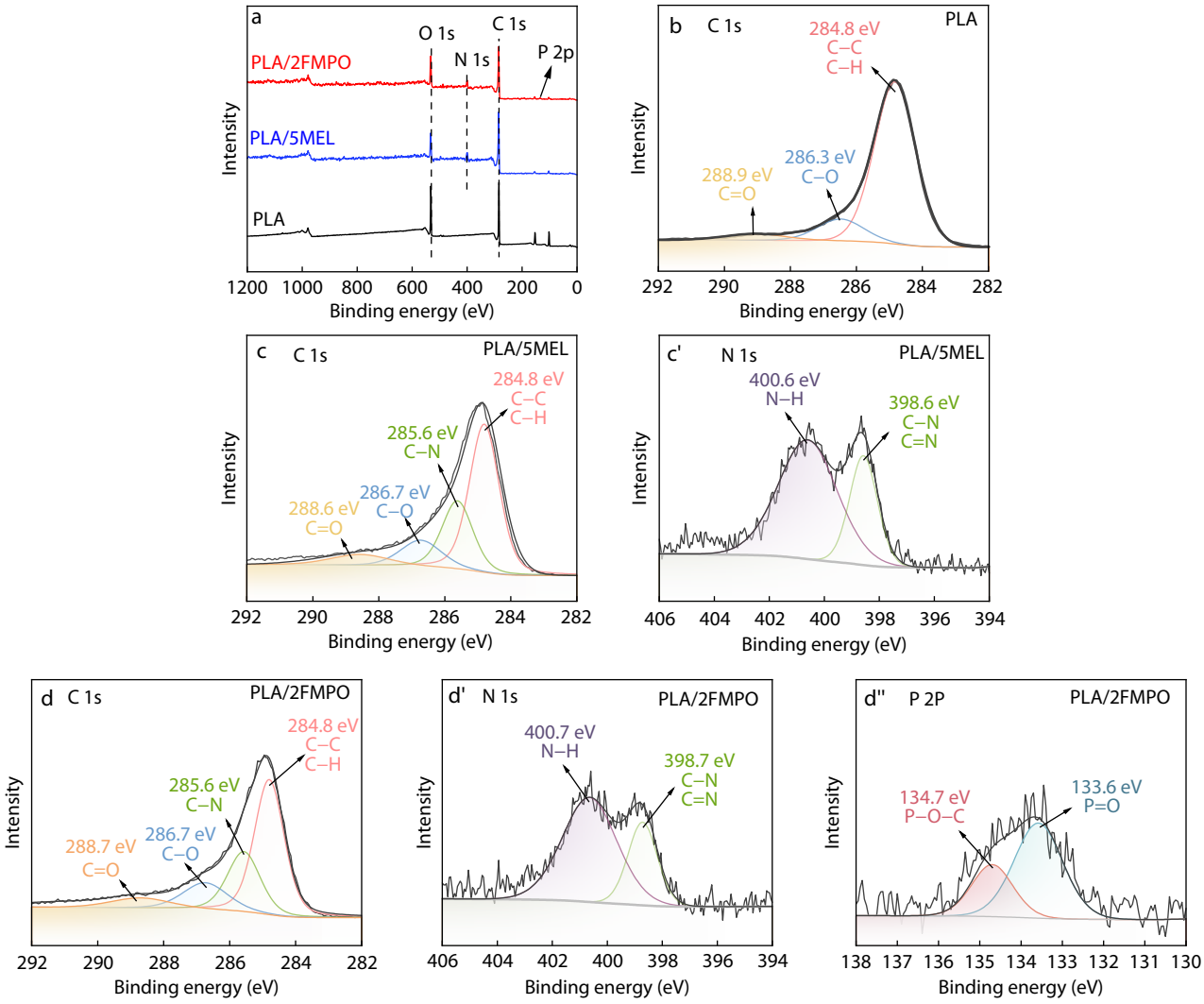

Fig. 7 XPS analysis of char residues from PLA composites: XPS full spectra (a); XPS high-resolution spectra of pure PLA: C 1s (b); PLA/5MEL: C 1s (c), N 1s (c'); PLA/2FMPO: C 1s (d), N 1s (d'), P 2p (d'').

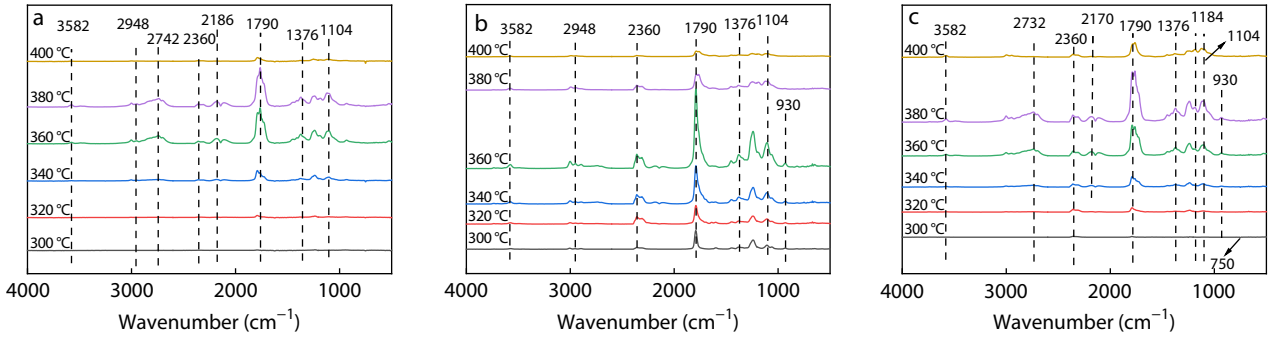

Fig. 8 FTIR spectra of pyrolysis products at different temperature stages of (a) PLA, (b) PLA/5MEL, (c) PLA/2FMPO.

mechanism for the PLA/FMPO system was proposed, as schematically illustrated in Scheme 2. When MEL was added, large amounts of inert gases such as NH_3 and N_2 were generated. A portion of these gases was discharged into the atmosphere, thereby creating a dilution effect that lowered the level of both combustible gases and oxygen in the surrounding environment. The remaining gases were trapped within the solid phase, filling the entire carbon layer. Therefore, MEL exhibited good carbonization performance but low flame-retardant efficiency. Regarding the mechanism of PLA/FMPO, in addition to the dilution effect of inert gases, phosphorus-derived active species produced during thermal decomposition are released to quench the highly reactive radicals (H•, OH•) in the gas phase, thus suppressing combustion intensity by effectively

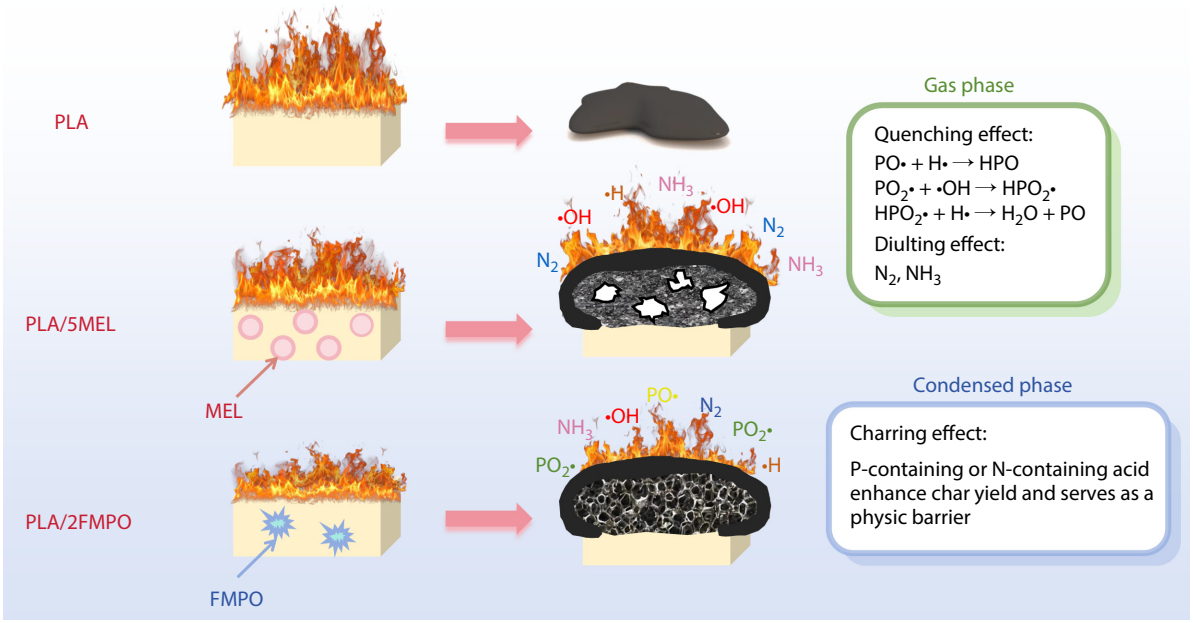

Scheme 2 Flame retardant mechanism diagram of PLA/FMPO.

Table 4 The mechanical properties of PLA composites.

Sample	Tensile strength (MPa)	Elongation at break (%)	Impact strength (kJ/m^2)
PLA	35.61	9.83	14.82
PLA/5MEL	18.22	3.97	5.46
PLA/1FMPO	21.02	4.83	27.26
PLA/2FMPO	22.93	6.40	13.81
PLA/3FMPO	23.08	8.86	12.08
PLA/4FMPO	24.32	9.03	12.32
PLA/5FMPO	25.79	9.12	12.92

terminating chain propagation reactions.[46,47] Moreover, the released phosphoric acid enhanced the robustness of the char layer, significantly improving its isolation effect. As a result, the flame-retardant efficacy of FMPO in both condensed phases and the gas is enhanced, so that the flame retardant efficiency of a small quantity of FMPO surpasses that of a large quantity of MEL.

Analysis of Mechanical Properties

PLA fractured in a completely brittle mode, exhibiting a high tensile strength (35.61 MPa) but a low impact strength (14.82 kJ/m^2). From the PLA/5MEL composites, the tensile strength, elongation at break and impact strength decreased by 48.8%, 59.6% and 63.2%, respectively, compared to those of neat PLA. This impairment is ascribed to the poor compatibility between MEL and PLA, where the excessive amount of flame retardant disrupts the homogeneous dispersion and interfacial compatibility, thereby weakening the interfacial adhesion in the composites. Unfortunately, the composite still suffered from mechanical degradation despite the incorporation of FMPO. However, according to the data in Table 4, the elongation at break and tensile strength of the composites gradually increase from PLA/1FMPO to PLA/5FMPO. The amino groups in the FMPO molecules reacted with PLA, while the incorporation of the DOPO structure enhanced the molecular polarity.[25] As a result, the toughness of the composites recovered to some extent with increasing FMPO content, though it remained lower than that of neat PLA. Notably, the impact strength of PLA/1FMPO was significantly higher than that of neat PLA. This suggests that at 1 wt% addition, FMPO induced a fundamental change in the fracture mechanism of PLA. The uniformly dispersed FMPO particles likely promoted extensive shear yielding in the matrix under high-speed impact, a process that absorbs substantial energy thereby enhancing the notched impact strength.

CONCLUSIONS

In this research, a phosphorus-nitrogen flame-retarding additive (FMPO) was synthesized from DOPO, melamine, and formaldehyde (1:1 molar ratio) for application in PLA. The LOI value increased from 21.6% to 33.2% at higher flame-retardant loadings. Notably, even at a low additive content, the impact resistance of PLA/1FMPO was significantly improved, and at the maximum loading, the impact strength showed only a moderate reduction of approximately 12% relative to neat PLA. Through comprehensive investigation of the thermal decomposition products and residual char, it was established that FMPO demonstrated notable effectiveness in both gaseous inhibition and condensed-phase action. This excellent flame retardancy is primarily due to the inert gas dilution, free radical scavenging within the gaseous phase, and the thermal shielding

performance of the carbon barrier within the condensed phase. This study demonstrated an efficient modification strategy for PLA, thereby offering an innovative solution for the development of sustainable materials that integrate both fire safety and environmental compatibility. Future studies could extend the application of FMPO to other polymer systems to validate the universality and potential of this molecular design strategy.

Conflict of Interests

The authors declare no interest conflict.

Data Availability Statement

The data supporting the findings of this study are available from the corresponding author upon reasonable request.

ACKNOWLEDGMENTS

The authors gratefully acknowledge the financial support of the Guizhou Normal University. This work was financially supported by the National Natural Science Foundation of China (No. 51763005).

REFERENCES

1 Xu, Y.; Zhang, W.; Qiu, Y.; Xu, M.; Li, B.; Liu, L. Preparation and mechanism study of a high efficiency bio-based flame retardant for simultaneously enhancing flame retardancy, toughness and crystallization rate of poly(lactic acid). *Compos. Part B Eng.* **2022**, *238*, 109913.
2 Ling, M.; Yin, N.; Chen, Y.; Zhou, Z.; Chen, H.; Dai, C.; Huang, J.; Zhang, W. Construction of polylactic acid-based flame retardant composites by zinc oxide and bamboo carbon. *Carbon Lett.* **2024**, *34*, 665–675.
3 Wu, N.; Fu, G.; Yang, Y.; Xia, M.; Yun, H.; Wang, Q. Fire safety enhancement of a highly efficient flame retardant poly(phenylphosphoryl phenylenediamine) in biodegradable poly(lactic acid). *J. Hazard. Mater.* **2019**, *363*, 1–9.
4 Zhu, G.; Gao, J.; Zhu, Z. Rational design of across-linked fully biobased flame retardant for high-efficiency fire safety and multifunctional enhancement in polylactic acid composites. *ACS Sustainable Chem. Eng.* **2025**, *13*, 7318–7331.
5 Nisar, M.; Santos, L. M. D.; Ullah, H.; Galland, G. B.; Geshev, J.; Bergmann, C.; Quijada, R. Poly(lactide) and Ni nanoparticles supported thermally reduced graphene oxide nanoarchitecture for magnetic stimuli-responsive material. *Polym. Compos.* **2025**, *46*, 11509–11525.
6 Russo, S.; Ferrentino, N.; Santulli, F.; Paul, G.; Lamberti, M.; Mazzeo, M.; Venditto, V.; Marchese, L.; Pappalardo, D. Circular strategies for polylactic acid waste: a pathway to advanced thermosets. *ACS Sustainable Chem. Eng.* **2025**, *13*, 15331–15341.
7 Gong, W.; Fan, M.; Luo, J.; Liang, J.; Meng, X. Effect of nickel phytate on flame retardancy of intumescent flame retardant polylactic acid. *Polym. Adv. Technol.* **2020**, *32*, 1548–1559.
8 Ma, M.; Jiang, Z.; Liu, Z.; Huang, B.; Sun, N.; Chen, S.; Shi, Y.; He, H.; Zhu, Y.; Wang, X. Toward flame retardancy, antimelt dripping, and UV resistance properties of polylactic acid based on eco-friendly core-shell flame retardant. *ACS Appl. Polym. Mater.* **2024**, *6*, 3814–3825.
9 Ozah, R.; Kumar, J. V. S. P.; Anand, S. H.; Kumar, C. R. Experimental investigation on mechanical, flammability, wear and thermal properties of 3D printed polylactic acid composite contain rice husk ash Si_3N_4 nanoparticle. *J. Aust. Ceram. Soc.* **2025**, *61*, 1211–1222.
10 Pasha, H. Y.; Mohtasebi, S. S.; Taherimehr, M.; Tabatabaeekoloor, R.; Firouz, M. S.; Javadi, A. New poly(lactic acid)-based

Graphical Abstract

A Phosphorus/Nitrogen-containing Phosphaphenanthrene Derivative as Flame Retardant for Poly(lactic acid)

Shan Lin, Hong-Yan Zhu, Chun-Meng You, and Da-Ming Ban

Guizhou Normal University

A phosphorus-nitrogen flame retardant (FMPO) was synthesized, which endows poly(lactic acid) with high flame retardancy at a low loading, exhibiting synergistic gas-phase and condensed-phase flame-retardant effects.

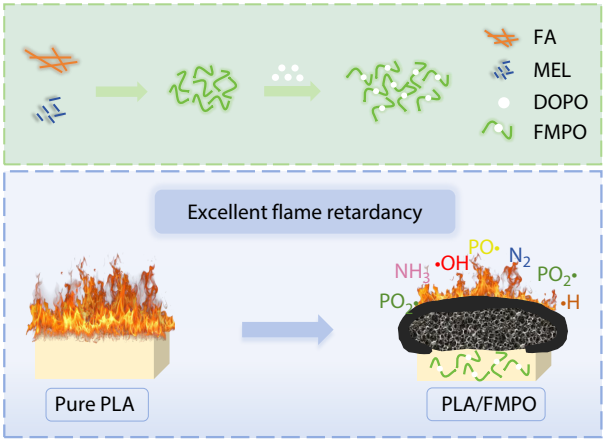

Chinese J. Polym. Sci. 2026, 44, 2282–2293 *https://doi.org/10.1007/s10118-026-3634-5*

nanocomposite films for food packaging applications. *Iran. Polym. J.* **2023**, *32*, 855–871.
11 Zhong, W.; Xu, P.; Niu, D.; Wang, Q.; Yang, W.; Zhang, X.; Liu, T.; Ma, P. Enhanced flame retardancy, ultraviolet shielding, and preserved mechanical properties of polylactic acid with fully biobased multifunctional additives by a green method. *ACS Sustain. Chem. Eng.* **2024**, *12*, 4017–4027.
12 Jia, L.; Zhang, W. C.; Tong, B.; Yang, R. J. Crystallization, mechanical and flame-retardant properties of poly(lactic acid) composites with DOPO and DOPO-POSS. *Chinese J. Polym. Sci.* **2018**, *36*, 871–879.
13 Baochai, L.; Bakar, A. A.; Mohamad, Z. An overview of the recent advances in flame retarded poly(lactic acid). *Polym. Adv. Technol.* **2023**, *34*, 1435–1450.
14 Li, B.; Sun, H.; Zhang, L.; Zhao, X.; Bakar, A. A.; Mohamad, Z. Flame-retarded poly (lactic acid) containing phosphating chitosan. *Fire Mater.* **2024**, *49*, 173–183.
15 Liu, Y.; Liu, Y.; Yang, R. Polylactic acid flame-retarded by nano-compound of form II ammonium polyphosphate with montmorillonite. *J. Fire Sci.* **2021**, *39*, 495–511.
16 Yuqin, Z.; Di, W.; Zhongliang, G.; Huiying, W. Performance analysis and structure characterization of polylactic acid modified with three flame retardants. *New J. Chem.* **2024**, *48*, 7469–7479.
17 Zheng, R.; Chen, Y.; Sun, Z.; Zhang, J.; Deng, Y.; Xu, X. Jute woven fabric modified by phosphorus-containing organosilicon compound reinforced flame retardant polylactic acid composites with enhanced flame retardant and mechanical properties. *Polym. Adv. Technol.* **2023**, *34*, 3617–3630.
18 Ma, C.; Yu, B.; Hong, N.; Pan, Y.; Hu, W.; Hu, Y. Facile synthesis of a highly efficient, halogen-free, and intumescent flame retardant for epoxy resins: thermal properties, combustion behaviors, and flame-retardant mechanisms. *Ind. Eng. Chem. Res.* **2016**, *55*, 10868–10879.
19 Yemisci, F.; Yesil, S.; Aytac, A. Improvement of the flame retardancy of plasticized poly(lactic acid) by means of phosphorus-based flame retardant fillers. *Fire Mater.* **2017**, *41*, 964–972.
20 Long, L.; Nie, X.; Wang, X.; Shan, C.; Qin, S.; Gong, W.; Hai, F.; Yu, J. Properties and mechanism of flame retardant poly(lactic acid) composites containing phosphaphenanthrene-hydroxyl phenyl maleimide derivative. *J. Polym Sci.* **2025**, *63*, 1695–1706.
21 Gu, L.; Qiu, J.; Sakai, E. Effect of DOPO-containing flame retardants on poly(lactic acid): non-flammability, mechanical properties and thermal behaviors. *Chem. Res. Chin. Univ.* **2017**, *33*, 143–149.
22 Zhang, D.; Pei, M.; Wei, K.; Tan, F.; Gao, C.; Bao, D.; Qin, S. Flame-retardant properties and mechanism of polylactic acid-conjugated flame-retardant composites. *Front. Chem.* **2022**, *10*, 894112.
23 Pei, M.; Wei, K.; Zhang, D.; Qin, S. Polylactic acid flame-retardant composite preparation and investigation of flame-retardant characteristics. *Polym. Eng. Sci.* **2023**, *63*, 880–894.
24 Yang, X.-M.; Qiu, S.; Yusuf, A.; Sun, J.; Zhai, Z.; Zhao, J.; Yin, G.-Z. Recent advances in flame retardant and mechanical properties of polylactic acid: a review. *Int. J. Biol. Macromol.* **2023**, *243*, 125050.
25 Wang, X.; He, W.; Long, L.; Huang, S.; Qin, S.; Xu, G. A phosphorus- and nitrogen-containing DOPO derivative as flame retardant for polylactic acid (PLA). *J. Therm. Anal. Calorim.* **2020**, *145*, 331–343.
26 Vakili, M.; Alavi Nikje, M. M.; Hajibeygi, M.; Vahabi, H. A reactive melamine-DOPO based flame retardant for superior thermal stability and flame retardancy in rigid polyurethane foam. *J. Elastomers Plast.* **2024**, *57*, 58–79.
27 Rao, W.-H.; Hu, Z.-Y.; Xu, H.-X.; Xu, Y.-J.; Qi, M.; Liao, W.; Xu, S.; Wang, Y.-Z. Flame-retardant flexible polyurethane foams with highly efficient melamine salt. *Ind. Eng. Chem. Res.* **2017**, *56*, 7112–7119.
28 Yan, Y.; Liang, B. Flame-retardant behavior and mechanism of a DOPO-based phosphorus-nitrogen flame retardant in epoxy resin. *High Perform. Polym.* **2018**, *31*, 885–892.
29 Zhang, Q.; Yang, S.; Wang, J.; Cheng, J.; Zhang, Q.; Ding, G.; Hu, Y.; Huo, S. A DOPO based reactive flame retardant constructed by multiple heteroaromatic groups and its application on epoxy resin: curing behavior, thermal degradation and flame retardancy. *Polym. Degrad. Stabil.* **2019**, *167*, 10–20.
30 Wang, C.; Ren, B.; Ma, R.; Li, X. A bio-based reactive P/N synergistic flame retardant for improving the fire safety and mechanical properties of epoxy resin. *Polym. Eng. Sci.* **2024**, *64*, 4730–4745.
31 Chen, R.; Hu, K.; Tang, H.; Wang, J.; Zhu, F.; Zhou, H. A novel flame retardant derived from DOPO and piperazine and its application in epoxy resin: flame retardance, thermal stability and pyrolysis behavior. *Polym. Degrad. Stabil.* **2019**, *166*, 334–343.
32 Chen, R.; Dongmei, B.; Jiang, J.; Sun, C.; Chen, H.; Zhang, M. Effect of 3-methoxysalicylaldehyde on transparency and mechanical properties of EP modified with aminopyridine-based DOPO derivative. *High Perform. Polym.* **2022**, *35*, 401–411.
33 Xi, W.; Qian, L.; Qiu, Y.; Chen, Y. Flame-retardant behavior of bi-group molecule derived from phosphaphenanthrene and triazine groups on polylactic acid. *Polym. Adv. Technol.* **2016**, *27*, 781–788.
34 Ran, G.; Liu, X.; Guo, J.; Sun, J.; Li, H.; Gu, X.; Zhang, S. Improving the flame retardancy and water resistance of polylactic acid by introducing polyborosiloxane microencapsulated ammonium polyphosphate. *Compos. Part B Eng.* **2019**, *173*, 106772.
35 Hou, B. Y.; Wang, Y. N.; Gong, T. Y.; Wang, R.; Huang, L. P.; Li, B. J.; Li, J. C. Fabrication of highly efficient biodegradable oligomeric lactate flame-retardant plasticizers for ultra-flexible flame-retardant poly (lactic acid) composites. *Chem. Eng. J.* **2024**, *485*, 149932.
36 Liu, T.; Jing, J.; Zhang, Y.; Fang, Z. Synthesis of a novel polyphosphate and its application with APP in flame retardant PLA. *RSC Adv.* **2018**, *8*, 4483–4493.
37 Ran, S.; Fang, F.; Guo, Z.; Song, P.; Cai, Y.; Fang, Z.; Wang, H. Synthesis of decorated graphene with P, N-containing compounds and its flame retardancy and smoke suppression effects on polylactic acid. *Compos. Part B Eng.* **2019**, *170*, 41–50.
38 Yu, S.; Xiang, H.; Zhou, J.; Zhu, M. Enhanced flame-retardant performance of poly (lactic acid) (PLA) composite by using intrinsically phosphorus-containing PLA. *Prog. Nat. Sci.: Mater. Int.* **2018**, *28*, 590–597.
39 Gao, D.; Wen, X.; Guan, Y.; Czerwonko, W.; Li, Y.; Gao, Y.; Mijowska, E.; Tang, T. Flame retardant effect and mechanism of nanosized NiO as synergist in PLA/APP/CSi-MCA composites. *Compos. Commun.* **2020**, *17*, 170–176.
40 Meng, Q.; Liu, X.; Li, S.; Wang, K.; Chen, L.; Wu, B.; Han, S. Silane-grafted black phosphorus nanosheets via ball milling: simultaneously enhanced flame retardancy and mechanical properties in polyurea composites. *React. Funct. Polym.* **2026**, *218*, 106549.
41 Hou, B.; Shan, X.; Li, B.; Zhang, Y.; Xu, B.; Cui, Q.; Chen, Z.; Li, J. Constructing novel biobased phosphorus-containing oligomeric lactates toward synchronously enhancing the toughness and fire safety of poly(lactic acid). *ACS Sustain. Chem. Eng.* **2024**, *12*, 6748–6761.
42 Wang, Y.; Zhang, Y.; Ma, L.; Gao, J.; Ge, H.; Zhu, Z. Layered charring agent with super strong carbonization for IFR system: achieving highly efficient flame retardancy of PLA by ultra-low addition IFR. *Sustain. Mater.Technol.* **2024**, *40*, e00924.
43 Jiang, P.; Zhang, S.; Bourbigot, S.; Chen, Z.; Duquesne, S.; Casetta,

M. Surface grafting of sepiolite with a phosphaphenanthrene derivative and its flame-retardant mechanism on PLA nanocomposites. *Polym. Degrad. Stabil.* **2019**, *165*, 68–79.
44 Jia, Y.-W.; Zhao, X.; Fu, T.; Li, D.-F.; Guo, Y.; Wang, X.-L.; Wang, Y.-Z. Synergy effect between quaternary phosphonium ionic liquid and ammonium polyphosphate toward flame retardant PLA with improved toughness. *Compos. Part B Eng.* **2020**, *197*, 108192.
45 Xu, H.; Song, X.; Chen, D.; Chen, J.; Wang, Y.; Shi, J.; Yang, J.; Liu, L. Green vanillin coupled with P/N/Si flame retardant for poly (L-lactic acid). *Mater. Today Commun.* **2024**, *39*, 108553.
46 Zhan, W.; Li, L.; Chen, L.; Kong, Q.; Chen, M.; Chen, C.; Zhang, Q.; Jiang, J. Biomaterials in intumescent fire-retardant coatings: a review. *Prog. Org. Coat.* **2024**, *192*, 108483.
47 Liu, L.; Xu, Y.; Di, Y.; Xu, M.; Pan, Y.; Li, B. Simultaneously enhancing the fire retardancy and crystallization rate of biodegradable polylactic acid with piperazine-1,4-diylbis(diphenylphosphine oxide). *Compos. Part B Eng.* **2020**, *202*, 108407.

https://doi.org/10.1007/s10118-026-3634-5